Theory of Dynamic Imaging of Molecules with intense infrared laser pulses

C. D. Lin, Anh-Thu Le and Zhangjin Chen

When a molecule is exposed to an intense laser pulse, electrons that are removed earlier in the laser field may be driven back by the oscillating electric field of the laser to recollide with the target ion. The scattering of the returning electrons offers the opportunities to study the structure of the molecule. Since lasers of pulse duration of a few femtoseconds are already available, thus it is possible to use few femtoseconds lasers for dynamic imaging of transient molecules. The basic scattering theories for dynamic quantum imaging of molecules are discussed.

1 Introduction

Imaging, or the determination of the structure of an object, has always played an important role in physical sciences. For microscopic systems, X-ray and electron diffraction are the conventional methods for achieving spatial resolutions on the order of Angstrom or less [1]. These methods, however, are not suitable for following the time evolution of a dynamic system, in particular, in a chemical reaction, which requires temporal resolutions of a few femtoseconds [2]. Although ultrafast electron diffraction (UED) and X-ray free-electron lasers (XFEL) that have come online and others being developed at big facilities are aiming at achieving temporal as well as spatial resolutions, it is important to investigate the possibilities of accomplishing

C. D. Lin
Department of Physics, Cardwell Hall, Kansas State University, Manhattan, KS 66506, USA e-mail: cdlin@phys.ksu.edu

Anh-Thu Le
Department of Physics, Cardwell Hall, Kansas State University, Manhattan, KS 66506, USA e-mail: atle@phys.ksu.edu

Zhangjin Chen
Department of Physics, Cardwell Hall, Kansas State University, Manhattan, KS 66506, USA e-mail: zjchen@phys.ksu.edu

the same goal using small-scale methods. In this contribution, we propose such an approach based on infrared or mid-infrared (MIR) lasers for dynamic imaging of molecules. Today such lasers have pulse durations of a few femtoseconds already, thus if they can reach good spatial resolution, then in principle these lasers can be used for dynamic imaging of molecules.

To study the structure of a molecule, the first step is to determine the bonding lengths and bond angles of all the atoms in the molecule. This is what the X-ray diffraction and electron diffraction are good for. For objects that can be crystallized X-ray diffraction is preferred. For molecules in the gas phase, electron diffraction is the standard method. The knowledge of bond lengths and bond angles (the geometry) in a molecule alone do not offer the full knowledge of the "chemistry" of a molecule, in particular, the bonding of the outer-shell electrons, as well as how the molecule will respond to an external perturbation. To probe the molecules at the next higher level, again electrons and photons are used. Thus electron-molecule scattering where electrons with energies from a few eV's to hundreds of eV's are used. Similarly, photons from ultraviolet to soft X-rays are used to probe the outershells of molecules. To understand the results of these measurements, advanced quantum mechanical many-body theories are needed since the effects of exchange and electron correlation are known to play important roles in such situations. A large fraction of modern atomic and molecular physics since the 1960's are devoted to these latter topics. Many powerful experimental and theoretical tools have been developed and a great deal of data base for each species have been documented. They form an essential component of our present knowledge of the microscopic world.

Infrared or MIR lasers have wavelengths from fractions to a few microns. They are much longer than the typical interatomic separations in a molecule. However, when a molecule is exposed to a short infrared laser pulse, electrons that were removed at an early time of the pulse may be driven back by the oscillating electric field of the laser to recollide with the molecular ion, to incur processes like high-order harmonic generation (HHG), high-energy above-threshold-ionization (HATI) electrons and nonsequential double ionization (NSDI). According to the rescattering model [3, 4], they are similar to conventional electron collision processes with the molecular ions. Thus HHG is due to the photo-recombination of the returning electrons with the molecular ion with the emission of high energy photons, i.e., a time-reversed process of photoionization of a neutral molecule. Similarly, HATI spectra are due to the elastic scattering of the returning electrons with the target ion for which the electrons are scattered into the backward directions, while NSDI is due to the impact ionization by the returning electrons with the emission of another electron similar to the (e, 2e) processes. Unlike low-energy electrons that are removed by the tunneling process which occurs far away from the core of the molecule, these rescattering processes are by fast electrons which have been accelerated by the laser field and the collisions occur close to the molecules. The energy of the returning electron is proportional to the laser intensity, and increases quadratically with the wavelength of the laser. Thus for a linearly polarized Ti-Sapphire laser with wavelength of 800 nm and peak intensity of 2×10^{14} W/cm^2, the maximum returning electron energy is about 38 eV. Using a MIR laser at wavelength of 1200 nm and

1800 nm, at the same peak intensity, the returning energy will be about 86 eV and 192 eV, respectively. Thus using IR or MIR lasers for probing the structure of a molecule, we rely on electron scattering. With the returning electron energies of 86 eV and 192 eV, they have de Broglie wavelength of 1.42 and 0.64 Angstroms, respectively. They are closer to the typical molecular size, making MIR lasers capable of probing the structure of a molecule.

The rescattering model or the so-called three-step model described above has been around since the early 1990's. However, they have always been used to "interpret" qualitatively the observed rescattering phenomena only. The model has not been put in a form for quantitative calculations. Recently we have developed a quantitative rescattering (QRS) theory [5, 6] which can be used to calculate HHG, HATI and NSDI yields. The applications of the QRS to these processes have been documented in a recent review article [6]. Essential to the QRS is the usual field-free scattering cross sections. For this book chapter, we will focus on the basic theories used in QRS instead of presenting many actual results. Thus, this article is written for those in the strong field community who are not familiar with quantum scattering theories. Clearly only the simple theories can be presented here. Advanced many-body scattering theories developed in the past half a century are beyond the reach of this contribution. Atomic units will be used in this article unless otherwise indicated.

2 Theoretical tools for studying atoms and molecules in strong fields

In this Section we present the elementary scattering theories for the solution of time-dependent and time-independent Schrödinger equations. These basic theoretical tools serve as the common language for both theorists and experimentalists in understanding the interaction of light or electrons with atoms and molecules.

2.1 Solution of the time-dependent Schrödinger equation

Based on quantum mechanics, the interaction of an intense laser pulse with an atom is described by the time-dependent Schrödinger equation (TDSE)

$$i\frac{\partial}{\partial t}\Psi(\mathbf{r},t) = H\Psi(\mathbf{r},t) \tag{1}$$

where

$$H = H_0 + H_i(t) = -\frac{1}{2}\nabla^2 + V(r) + H_i(t). \tag{2}$$

The atom-field interaction, in length gauge, is given by

$$H_i = \mathbf{r}\cdot\mathbf{E}(t), \tag{3}$$

where $\mathbf{E}(t)$ is the laser field. For simplicity, the atom is approximated by a model potential

$$V(r) = -\frac{1+a_1e^{-a_2r}+a_3re^{-a_4r}+a_5e^{-a_6r}}{r}, \tag{4}$$

where the parameters a_i's are obtained by fitting to the known energies of the ground state and the first few excited states of the atom. The model potential for a neutral atom can also be expressed as

$$V(r) = V_s(r) - 1/r, \tag{5}$$

where the Coulomb potential part is separated out and $V_s(r)$ is the remaining short-range potential. The TDSE can be solved by expanding $\Psi(\mathbf{r},t)$ in terms of eigenfunctions of H_0 within a box of $r \in [0, r_{max}]$

$$\Psi(\mathbf{r},t) = \sum_{nl} c_{nl}(t) R_{nl}(r) Y_{lm}(\hat{\mathbf{r}}) \tag{6}$$

where the radial functions $R_{nl}(r)$ are expanded using the DVR (discrete variable representation) basis functions associated with Legendre polynomials, while the c_{nl} are calculated using the split-operator method. At the end of the laser pulse $t = t_{end}$, the photoelectron yield is computed by projecting out the total wavefunction onto eigenstates of a continuum electron with momentum $\mathbf{k}$,

$$D(k,\theta) \equiv \frac{\partial^3 P}{\partial^3 \mathbf{k}} = |\langle \Phi_{\mathbf{k}}^- | \Psi(t = t_{end})\rangle|^2 \tag{7}$$

where the continuum state $\Phi_{\mathbf{k}}^-$ satisfies the following equation

$$\left[-\frac{1}{2}\nabla^2 + V(r)\right]\Phi_{\mathbf{k}}^- = \frac{k^2}{2}\Phi_{\mathbf{k}}^-. \tag{8}$$

Here $\Phi_{\mathbf{k}}^-$ satisfies the incoming wave boundary condition. It can be expanded in terms of partial waves as

$$\Phi_{\mathbf{k}}^-(\mathbf{r}) = \frac{1}{\sqrt{k}}\sum_{lm} i^l \exp[-i(\sigma_l+\delta_l)] R_{El}(r) Y_{lm}(\hat{\mathbf{r}}) Y_{lm}^*(\hat{\mathbf{k}}). \tag{9}$$

Here, δ_l is the l-th partial wave phase shift due to the short range potential $V_s(r)$ in Eq. (5), and σ_l is the Coulomb phase shift. The Y's are the usual spherical harmonics. For the continuum radial function R_{El}, it is energy normalized such that

$$\int_0^\infty R_{El}(r)R_{E'l}(r)r^2dr = \delta(E-E'), \tag{10}$$

and has the asymptotic form

$$R_{El}(r) \to \frac{1}{r}\sqrt{\frac{2}{\pi k}}\sin(kr - l\pi/2 - \gamma\log 2kr + \sigma_l + \delta_l). \tag{11}$$

The details of such calculations can be found in [7].

2.2 Strong field approximation

In the strong field approximation (SFA), one treats the atomic potential as perturbation. In the first-order SFA, called SFA1 here, the ionization of the atom is calculated from

$$f_1(\mathbf{k}) = -i\int_{-\infty}^{\infty} dt \left\langle \chi_{\mathbf{k}}(t)\left|H_i(t)\right|\Psi_0(t)\right\rangle. \tag{12}$$

Here Ψ_0 is the initial state, H_i is the laser-electron interaction and $\chi_{\mathbf{k}}$ is the Volkov state. To describe rescattering, a second-order SFA (SFA2) [8, 9, 10] is needed. For SFA2, the scattering amplitude can be written as

$$\begin{aligned} f_2(\mathbf{k}) = &-\int_{-\infty}^{\infty} dt \int_t^{\infty} dt' \int d\mathbf{p} \left\langle \chi_{\mathbf{k}}(t')\left|V\right|\chi_{\mathbf{p}}(t')\right\rangle \\ &\times \left\langle \chi_{\mathbf{p}}(t)\left|H_i(t)\right|\Psi_0(t)\right\rangle. \end{aligned} \tag{13}$$

Here the electron is first ionized at time t and rescattered at time t'. The potential V is the electron-ion interaction, i.e., the model potential chosen. Integration over the momentum is carried out using saddle-point approximation.

2.3 Laser-free elastic scattering theory

In quantum mechanics, the scattering of an electron by a spherically symmetric potential $V(r)$ is governed by the time-independent Schrödinger equation

$$[\nabla^2 + k^2 - U(r)]\psi(\mathbf{r}) = 0 \tag{14}$$

where $U(r) = 2V(r)$ is the reduced potential and k is the electron momentum, related to the incident electron energy by $k = \sqrt{2E}$. For a short-range potential which tends to zero faster then r^{-2} as $r \to \infty$, the scattering wave function satisfies the asymptotic outgoing wave boundary condition

$$\psi^+(\mathbf{r})_{r\to\infty} = \frac{1}{(2\pi)^{3/2}}\left[\exp(ikz) + f(\theta)\frac{\exp(ikr)}{r}\right] \tag{15}$$

where θ is the polar angle measured from the incident direction. We choose the z-axis along the direction of the incident wave vector $\mathbf{k}$. Here $\psi^+(\mathbf{r})$ satisfies the outgoing wave boundary condition and can be expanded in terms of partial waves,

$$\psi^+(\mathbf{r}) = \sqrt{\frac{2}{\pi}}\frac{1}{kr}\sum_{lm} i^l e^{i\delta_l} u_l(kr) Y_{lm}(\hat{\mathbf{r}}) Y^*_{lm}(\hat{\mathbf{k}}) \tag{16}$$

where Y_{lm} is a spherical harmonic. The continuum waves are normalized to $\delta(\mathbf{k}-\mathbf{k}')$. The radial function $u_l(kr)$ satisfies

$$\left[\frac{d^2}{dr^2} + k^2 - \frac{l(l+1)}{r^2} - U(r)\right] u_l(kr) = 0. \tag{17}$$

The above expressions are valid for short-range potential only. For a Coulomb potential, $V_c = -Z/r$, its full wavefunction can be expanded as

$$\psi_c^+(\mathbf{r}) = \sqrt{\frac{2}{\pi}}\frac{1}{kr}\sum_{lm} i^l e^{i\sigma_l} u_l^c(kr) Y_{lm}(\hat{\mathbf{r}}) Y^*_{lm}(\hat{\mathbf{k}}) \tag{18}$$

where

$$\sigma_l = \arg[\Gamma(l+1+i\eta)] \tag{19}$$

is called the Coulomb phase shift with $\eta = -Z/k$. The scattering amplitude for the Coulomb potential can be obtained analytically using parabolic coordinates,

$$f_c(\theta) = -\eta\exp(2i\sigma_0)\frac{\exp\{-i\eta\ln[\sin^2(\theta/2)]\}}{2k\sin^2(\theta/2)}. \tag{20}$$

The atomic potential in Eq. (5) is an example of modified Coulomb potential. In such a potential the scattering amplitudes is the sum of Coulomb scattering amplitude and the amplitude from the short-range potential alone

$$f(\theta) = f_c(\theta) + \hat{f}(\theta), \tag{21}$$

where the first term is the Coulomb scattering amplitude [Eq. (20)], and the second term is given by

$$\hat{f}(\theta) = \sum_{l=0}^{\infty}\frac{2l+1}{k}\exp(2i\sigma_l)\exp(i\delta_l)\sin\delta_l P_l(\cos\theta) \tag{22}$$

where $P_l(\cos\theta)$ is the Legendre polynomial, and δ_l is the phase shift from the short-range potential. Due to the short range nature, the summation in Eq. (22) can be

truncated after some number of partial waves, depending on the electron energy. The elastic scattering DCS is then given by

$$\sigma(k,\theta) \equiv \frac{dP}{d\Omega} = |f_c(\theta) + \hat{f}(\theta)|^2. \tag{23}$$

For high-energy scattering, if the scattering is treated to first-order, then the scattering cross section is given by the so-called plane wave Born approximation (PWBA) or first Born (B1) approximation. In B1, the DCS is calculated from

$$\sigma_{PWBA}(k,\theta) = \frac{1}{4\pi^2}|V(\mathbf{q})|^2 \tag{24}$$

i.e., proportional to the square of the potential in the momentum space. Here $\mathbf{q}$ is the momentum transfer and its magnitude is $q = 2k\sin(\theta/2)$. In B1 the continuum electron wavefunctions are represented by plane waves. For electron-target ion collisions, B1 is not valid even at large collision energies since it neglects the effect of long-range Coulomb interaction as well as the strong short-range potential due to the atomic ion or molecular ion core.

2.4 Quantitative rescattering theory

For a one-electron atom, we can solve TDSE to obtain the photoelectron momentum spectra $D(k,\theta)$. For a given model potential $V(r)$, one can also calculate accurate DCS, $\sigma(k_r,\theta_r)$, for a given k_r. Both can be obtained essentially "exactly". Since the rescattering model does not specify how to calculate the returning electron wave packet, we define it as the ratio

$$W(k_r,\theta_r) = D(k,\theta)/\sigma(k_r,\theta_r). \tag{25}$$

If the rescattering concept is correct, then the ratio should not depend on the angle θ_r. Before the ratio can be calculated, we need to establish the relation between (k,θ) and (k_r,θ_r). The k_r is the momentum value after electron is scattered by the ion. Since the collision occurs in the laser field, it is still under the influence of the laser after the collision. As it exits from the laser field, an additional momentum along the direction of the laser polarization will be added. Thus we can write

$$k_z = k\cos\theta = \pm A_r \mp k_r\cos\theta_r, \tag{26}$$

$$k_y = k\sin\theta = k_r\sin\theta_r. \tag{27}$$

The upper signs in Eq. (26) refer to the right-side ($k_z > 0$) while the lower ones to the left-side ($k_z < 0$) electrons. Here A_r=$A(t_r)$ is the vector potential at the time t_r of collision. Note that the electron can return from the left or the right along the polarization axis to revisit the target ion. Based on the classical rescattering theory,

the returning momentum k_r is related to the vector potential A_r by $A_r = k_r/1.26$. Note that this sets the maximum returning electron energy at 3.2 U_p. Here U_p is the ponderomotive energy, $U_p = I/4\omega^2$, with ω the angular frequency of the laser and I the peak intensity. With these conditions, we then solve

$$\tan\theta = \frac{\sin\theta_r}{\pm(1/1.26 - \cos\theta_r)}, \tag{28}$$

$$k^2 = k_r^2(1.63 - 1.59\cos\theta_r) \tag{29}$$

These two expressions relate the momentum of the photoelectron and the momentum of the electron in the field after elastically rescattered by the ion.

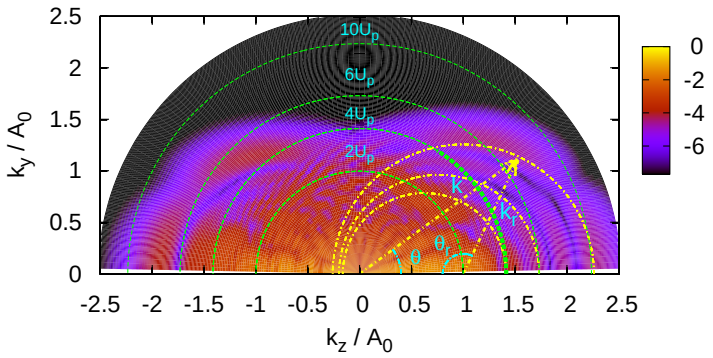

Fig. 1 Typical 2D electron momentum distributions (in logarithmic scale): The TDSE calculation is for single ionization of Ar in a 5 fs laser pulse at the intensity of 1.0×10^{14} W/cm^2 with the wavelength of 800 nm. Photoelectrons of a given energy are represented on a concentric circle centered at the origin. The elastic scattering of a returning electron with momentum k_r in the laser field is represented by a partial circle with its center shifted from the origin by $A_r = k_r/1.26$.

2.5 The rescattering electron wave packet

In Fig. 1 the relation between the two momentum vectors are shown. Take the photoelectron yield along the semicircle of k_r=constant and divide it by the DCS, $\sigma(k_r, \theta_r)$, we obtain $W(k_r, \theta_r)$. Examples of such $W(k_r, \theta_r)$ are shown in Fig. 2. For the upper frame ones, they are obtained from TDSE solutions and the exact DCS. We note that $W(k_r, \theta_r)$ does not depend on θ_r, thus we can drop the dependence on θ_r and write it as $W(k_r)$. This condition is essential if we are to call $W(k_r)$ a

wave packet as in typical scattering theory. Note how $W(k_r)$ was defined. It is not a measurable quantity since it is defined when the laser field is still on. Using SFA2, we can obtain a similar wave packet. Here the DCS is taken from $\sigma_{PWBA}(k_r,\theta_r)$, Eq. (24). Since in SFA2 the electron-ion interaction is treated to first order only, thus the PWBA cross section should be used for $\sigma(k_r,\theta_r)$. We note that the resulting $W(k_r)$ from SFA2, shown in the bottom row of Fig. 2, are essentially identical to the ones on the upper row. We comment that only the k_r-dependence of the wave packet is considered here. Their absolute values are different, reflecting that the ionization rates from TDSE and from SFA are different.

The $W(k_r)$ obtained from SFA2 and from TDSE are identical is the most profound result of the QRS model. In fact, in hindsight, it should be expected if the rescattering picture is valid. After tunneling ionization, the motion of the electron is mostly away from the atomic ion. Thus $W(k_r)$ is determined mostly by the interaction of a free electron with the laser field. This interaction is treated exactly in SFA2, thus the $W(k_r)$ from SFA2 is very close to the one from TDSE. In SFA2, the tunneling ionization rate is not calculated correctly, nor the electron-ion scattering cross sections. The electron wave packet, $W(k_r)$, however, is accurate. Thus in the quantitative rescattering (QRS) theory, we can obtain HATI spectra from

$$D(k,\theta) = W(k_r)\sigma(k_r,\theta_r), \tag{30}$$

where $W(k_r)$ is the $W_{SFA}(k_r)$ calculated from SFA2. Since SFA2 calculations are much faster than solving TDSE, and the calculation of $\sigma(k_r,\theta_r)$ is the same as in field-free scattering cross sections, the QRS provides a very simple and accurate method of obtaining HATI spectra on the one hand, and on the other hand, allows one to extract field-free DCS, $\sigma(k_r,\theta_r)$, from experimental HATI spectra. The latter establishes the theoretical foundation for using infrared lasers for imaging the structure of a target. Since infrared lasers with pulse durations of a few femtoseconds are already available, it has the potential for dynamic chemical imaging with temporal resolution of a few femtoseconds.

The analysis so far concerns with the interaction of an atom with a laser of well-defined intensity. In actual experiments, an intense laser does not have fixed intensity within the focus volume. Thus to compare with experimental HATI spectra, theoretical calculations must include the volume effects [11]. For a peak intensity I_0 at the focal point, the yield of the photoelectrons with momentum $\mathbf{k}$ should be

$$S(\mathbf{k},I_0) = \rho \int_0^{I_0} D_I(k,\theta)\left(\frac{\partial V}{\partial I}\right) dI \tag{31}$$

where ρ is the density of atoms in the chamber, $D_I(k,\theta)$ denotes the momentum distribution for a single intensity I and $(\partial V/\partial I)dI$ represents the volume of an isointensity shell between I and $I+dI$.

In the QRS calculations, we obtain the volume-integrated returning electron wave packet using Eq. (31) since the DCS does not depend on the laser intensity. Consequently, Eq. (31) becomes

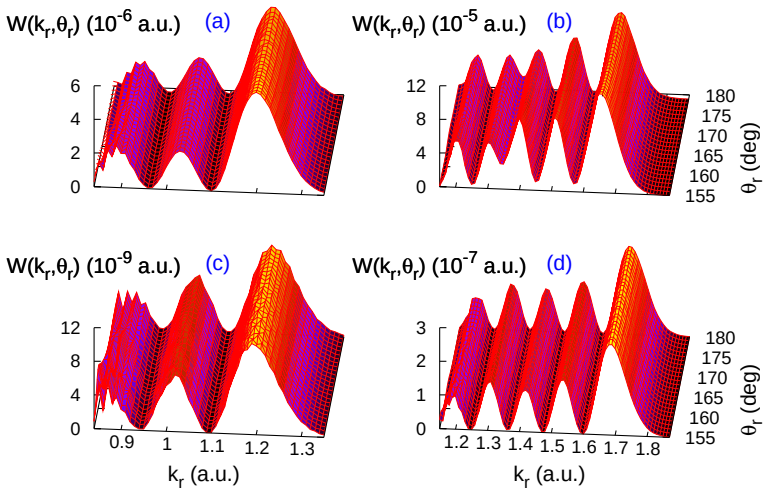

Fig. 2 (Color online) Right-side wave packets extracted from the electron momentum distributions calculated using TDSE and SFA2, for single ionization of Ar in a 5 fs laser pulse with the wavelength of 800 nm. Left column: from TDSE (top) and SFA2 (bottom), at intensity of 1.0×10^{14} W/cm^2; Right column: same, but at 2.0×10^{14} W/cm^2.

$$S(\mathbf{k}, I_0) = \bar{W}_{I_0}(k_r)\sigma(k_r, \theta_r) \tag{32}$$

where $\bar{W}_{I_0}(k_r)$ is the volume-integrated wave packet at the peak intensity I_0

$$\bar{W}_{I_0}(k_r) = \rho \int_0^{I_0} W_I(k_r) \left(\frac{\partial V}{\partial I}\right) dI \tag{33}$$

with $W_I(k_r)$ being the wave packet for the laser pulse at a single intensity I.

2.6 High-order Harmonic Generation

For the model one-electron atomic system, once the time-dependent wavefunction $\Psi(\mathbf{r},t)$ is obtained from solving Eq. (1), one can calculate the induced dipole of the atom by the laser field either in the length or acceleration forms

$$D_L(t) = \langle \Psi(\mathbf{r},t)|z|\Psi(\mathbf{r},t)\rangle \tag{34}$$

$$D_A(t) = \langle \Psi(\mathbf{r},t)|\frac{\partial V(r)}{\partial z}|\Psi(\mathbf{r},t)\rangle. \tag{35}$$

The HHG power spectra are obtained from Fourier components of the induced dipole moment $D(t)$ as given by

$$P(\omega) \propto |a(\omega)|^2 = \left| \int \frac{d^2 D(t)}{dt^2} e^{i\omega t} dt \right|^2 \approx \omega^4 |D(\omega)|^2. \tag{36}$$

Since TDSE cannot be solved accurately for molecular targets, the strong field approximation, or the SFA2, has been employed for obtaining HHG since the 1990's. Here we show SFA2 for molecular targets. Assuming that the molecules are aligned along the x-axis, in a laser field $E(t)$, linearly polarized on the x-y plane with an angle θ with respect to the molecular axis. The parallel component of the induced dipole moment can be written in the form

$$\begin{aligned} D_{\parallel}(t) = i \int_0^{\infty} d\tau \left(\frac{\pi}{\varepsilon + i\tau/2} \right)^{3/2} & [\cos\theta d_x^*(t) + \sin\theta d_y^*(t)] \\ & \times [\cos\theta d_x(t-\tau) + \sin\theta d_y(t-\tau)] E(t-\tau) \\ & \times \exp[-iS_{st}(t,\tau)] a^*(t) a(t-\tau) + c.c. \end{aligned} \tag{37}$$

where $\mathbf{d}(t) \equiv \mathbf{d}[\mathbf{p}_{st}(t,\tau) + \mathbf{A}(t)]$, $\mathbf{d}(t-\tau) \equiv \mathbf{d}[\mathbf{p}_{st}(t,\tau) + \mathbf{A}(t-\tau)]$ are the transition dipole moments between the ground state and the continuum state, and $\mathbf{p}_{st}(t,\tau) = -\int_{t-\tau}^{t} \mathbf{A}(t')dt'/\tau$ is the canonical momentum at the stationary points, with $\mathbf{A}$ the vector potential. The perpendicular component $D_{\perp}(t)$ is given by a similar formula with $[\cos\theta d_x^*(t) + \sin\theta d_y^*(t)]$ replaced by $[\sin\theta d_x^*(t) - \cos\theta d_y^*(t)]$ in Eq. (37). The action at the stationary points for the electron propagating in the laser field is

$$S_{st}(t,\tau) = \int_{t-\tau}^{t} \left(\frac{[\mathbf{p}_{st}(t,\tau) + \mathbf{A}(t')]^2}{2} + I_p \right) dt', \tag{38}$$

where I_p is the ionization potential of the molecule. In Eq. (37), $a(t)$ is introduced to account for the ground state depletion.

According to the rescattering model, HHG occurs when the returning electrons photo-recombine with the parent ions, with the emission of high-energy photons. Following the QRS, we can anticipate a relation similar to Eq. (30) for HHG [12]. Since the phase of the HHG is important, we write the *complex* laser-induced dipole as

$$|D(\omega)|e^{i\phi(\omega)} = |W(E)|e^{i\eta(E)}|d(\omega)|e^{i\delta(\omega)}, \tag{39}$$

where ϕ and η are the phases of the harmonic and the returning electron wave packet $W(E)$, respectively; d and δ are the amplitude and phase of the photo-recombination transition dipole. The electron energy E is related to the emitted photon energy ω by $E = \omega - I_p$, with I_p being the ionization potential of the target. Note that the W(E) defined here is the complex electron wave packet amplitude, whereas $W(k_r)$ defined for HATI electrons are the "intensity".

In the equation above the transition dipole is similar to the one used in photoionization theory. For the transition from an initial bound state Ψ_i to the final continuum state $\Psi_{\mathbf{k}}^-$ due to a linearly polarized light field (in the length form) it is given by

$$d_{\mathbf{k},\mathbf{n}}(\omega) = \langle \Psi_i | \mathbf{r} \cdot \mathbf{n} | \Psi_{\mathbf{k}}^- \rangle. \tag{40}$$

Here **n** is the direction of the light polarization and **k** is the momentum of the ejected photoelectron. For atomic targets, using the scattering wavefunction given by Eq. (9), we can evaluate the dipole transition matrix element. For example, for photoionization from the 3p shell of Ar, the transition dipole can be written as

$$\langle \Psi_i|z|\Psi_{\mathbf{k}}^+\rangle = \frac{1}{\sqrt{3\pi k}}\left[e^{i(\sigma_0+\delta_0)}\langle R_{31}|r|R_{E0}\rangle/2 - e^{i(\sigma_2+\delta_2)}\langle R_{31}|r|R_{E2}\rangle\right]. \quad (41)$$

For molecular targets, the calculation of the transition dipole is more complicated. Both the ground state and the continuum state wavefunctions have to be calculated using more advanced quantum chemistry packages. The photoionization differential cross section (DCS) can be expressed in the general form as

$$\frac{d^2\sigma^I}{d\Omega_{\mathbf{k}}d\Omega_{\mathbf{n}}} = \frac{4\pi^2\omega k}{c}\left|\langle \Psi_i|\mathbf{r}\cdot\mathbf{n}|\Psi_{\mathbf{k}}^-\rangle\right|^2, \quad (42)$$

where $k^2/2+I_p=\omega$ with I_p being the ionization potential, ω the photon energy, and c the speed of light. A more extended discussion for the calculation of the transition dipole moments of molecules can be found in Section II.D of Le *et al*. [12] where references to other works can be found as well.

2.7 Nonsequential double ionization due to the direct (e, 2e) collision processes

Nonsequential double ionization (NSDI) is another interesting rescattering phenomenon when atoms and molecules are placed in the laser field. NSDI involves at least two electrons. According to the rescattering picture, the returning electron can knock out another electron in a process similar to the electron impact ionization of an atom, or the so-called (e, 2e) process. Clearly Eq. (30) can be used to obtain the momentum distributions of the ionizing and the ejected electrons. Since electron impact ionization occurs in the laser field, the photoelectron momentum of each electron has to be shifted in the same way as in Eqs. (26) and (27). According to QRS, the main additional ingredient needed is the differential cross sections for the (e, 2e) collisions. Below we discuss the elementary field-free electron impact ionization theory.

Consider a two-electron atomic system. Let $\mathbf{r}_1$ and $\mathbf{r}_2$ be the position vectors of the projectile and the bound state electron, respectively, the exact Hamiltonian for the whole system is

$$H = -\frac{1}{2}\nabla_1^2 - \frac{Z_N}{r_1} - \frac{1}{2}\nabla_2^2 - \frac{Z_N}{r_2} + \frac{1}{r_{12}}. \quad (43)$$

This Hamiltonian can be rewritten approximately as

$$H_i = -\frac{1}{2}\nabla_1^2 + U_i(r_1) - \frac{1}{2}\nabla_2^2 - \frac{Z_N}{r_2} \tag{44}$$

where we assume that the He^+ ion initially is in the ground state, and the charge of the nucleus is $Z_N = 2$. Here $U_i(r_1)$ is the initial state distorting potential which is used to calculate the initial state wave function for the projectile. Using the prior form, the direct transition amplitude for the (e, 2e) collision process is

$$f_{e2e}(\mathbf{k}_1, \mathbf{k}_2) = \langle \Psi^-_{\mathbf{k}_1,\mathbf{k}_2} | V_i | \Psi_{\mathbf{k}_i} \rangle \tag{45}$$

where V_i is the perturbation interaction,

$$V_i = H - H_i = \frac{1}{r_{12}} - \frac{Z_N}{r_1} - U_i(r_1). \tag{46}$$

In (45), $\Psi^-_{\mathbf{k}_1,\mathbf{k}_2}$ is an exact solution of the three-body problem satisfying the incoming-wave boundary condition for two electrons with momentum vectors $\mathbf{k}_1$ and $\mathbf{k}_2$. There is no exact analytical solutions for $\Psi^-_{\mathbf{k}_1,\mathbf{k}_2}$, thus various approximations have to be used. First consider the so-called BBK model[13] which is expressed as

$$\begin{aligned}\Psi^-_{\mathbf{k}_1,\mathbf{k}_2}(\mathbf{r}_1, \mathbf{r}_2) = (2\pi)^{-3} \exp(i\mathbf{k}_1 \cdot \mathbf{r}_1) \exp(i\mathbf{k}_2 \cdot \mathbf{r}_2) \\ \times C(\alpha_1, \mathbf{k}_1, \mathbf{r}_1) C(\alpha_1, \mathbf{k}_2, \mathbf{r}_2) C(\alpha_{12}, \mathbf{k}_{12}, \mathbf{r}_{12}),\end{aligned} \tag{47}$$

where the Coulomb part of the wave function is defined as

$$C(\alpha, \mathbf{k}, \mathbf{r}) = \exp(-\pi\alpha/2)\Gamma(1 - i\alpha)\, {}_1F_1[i\alpha; 1; -i(kr + \mathbf{k} \cdot \mathbf{r})] \tag{48}$$

and

$$\begin{aligned}\mathbf{k}_{12} = \frac{1}{2}(\mathbf{k}_1 - \mathbf{k}_2), \quad \mathbf{r}_{12} = \mathbf{r}_1 - \mathbf{r}_2, \\ \alpha_1 = -\frac{Z_N}{k_1}, \quad \alpha_2 = -\frac{Z_N}{k_2}, \quad \alpha_{12} = \frac{1}{2k_{12}}.\end{aligned} \tag{49}$$

In (47), the Coulomb interaction between the two outgoing electrons has been taken into account. If we set $\alpha_{12} = 0$, then the electron-electron interaction is turned off and the two continuum electrons are then given by the product of two Coulomb functions, each electron seeing the charge Z_N from the nucleus. In the equation above, Γ is the gamma function and ${}_1F_1$ is the confluent hypergeometric function.

From the approximate initial state Hamiltonian H_i, we can write down the initial state wavefunction in the product form

$$\Psi_{\mathbf{k}_i}(\mathbf{r}_1, \mathbf{r}_2) = \varphi_{\mathbf{k}_i}(\mathbf{r}_1)\phi_{He^+}(\mathbf{r}_2) \tag{50}$$

where $\varphi_{\mathbf{k}_i}(\mathbf{r}_1)$ describes the incident electron and satisfies

$$\left[-\frac{1}{2}\nabla_1^2 + U_i(r_1) - \frac{1}{2}k_i^2\right]\varphi_{\mathbf{k}_i}(\mathbf{r}_1) = 0, \tag{51}$$

here $\mathbf{k}_i$ is the incident momentum and $\phi_{He^+}(\mathbf{r}_2)$ is the ground state wavefunction of He^+. Due to the energy conservation, the wave vectors k_1 and k_2 satisfy

$$\frac{1}{2}k_i^2 = \frac{1}{2}k_1^2 + \frac{1}{2}k_2^2 + I_p. \tag{52}$$

The discussion up to now assumes that the two electrons are distinguishable. Including the exchange, the triply differential cross section (TDCS) for the electron impact ionization process is given by

$$\frac{d^3\sigma_{e2e}}{d\Omega_1 d\Omega_2 dE} = (2\pi)^4 \frac{k_1 k_2}{k_i}\left[\frac{3}{4}|f_{e2e}(\mathbf{k}_1,\mathbf{k}_2) - g_{e2e}(\mathbf{k}_1,\mathbf{k}_2)|^2 + \frac{1}{4}|f_{e2e}(\mathbf{k}_1,\mathbf{k}_2) + g_{e2e}(\mathbf{k}_1,\mathbf{k}_2)|^2\right] \tag{53}$$

where $\Omega_1(\theta_1,\phi_1)$ and $\Omega_2(\theta_2,\phi_2)$ are the solid angles of detection of the two electrons leaving the collision with momenta $\mathbf{k}_1$ and $\mathbf{k}_2$, and $g_{e2e}(\mathbf{k}_1,\mathbf{k}_2)$ is the exchange amplitude with $g_{e2e}(\mathbf{k}_1,\mathbf{k}_2) = f_{e2e}(\mathbf{k}_2,\mathbf{k}_1)$.

The distortion potential $U_i(r_1)$ in (51) is not determined so far. If we choose $U_i(r_1) = 0$, then the incident electron is given by a plane wave. On the other hand, if the distortion potential is set as $U_i(r_1) = -(Z_N - 1)/r_1$, then it is described by a Coulomb wave. By calculating the TDCS using different approximate initial and final state wavefunctions, we can specify P-CC, P-CCC and C-CCC models for the (e, 2e) processes; here the first letter indicates a plane wave (P) or a Coulomb wave (C) for describing the incident electron, the second string of letters indicate that electron-electron repulsion is not included, in CC, or is included, in CCC. By comparing the results of such calculations with experimental measurement, the effect of Coulomb interaction between the two electrons can be assessed. Note that this effect depends on the kinetic energy, as well as the angle between the momentum vectors of the two electrons.

2.8 Nonsequential double ionization due to the indirect excitation-tunneling ionization processes

In NSDI, electron collision occurs in the laser field. If the core electron is excited by the returning electron to an excited state, the excited electron may be tunnel ionized by the laser field, resulting in the emission of two electrons. To calculate such processes, one first needs to obtain electron impact excitation cross sections, then evaluate the removal of the excited electron, where one can use the simple tunneling model.

For electron impact excitation, the final state wavefunction is given by

$$\Phi^{-}_{\mathbf{k}_f}(\mathbf{r}_1,\mathbf{r}_2) = \varphi^{-}_{\mathbf{k}_f}(\mathbf{r}_1)\phi_f(\mathbf{r}_2) \tag{54}$$

where $\varphi_{\mathbf{k}_f}$ is the wave function used to describe the outgoing electron, which satisfies the differential equation

$$\left(-\frac{1}{2}\nabla_1^2 + U_f(r_1)\right)\varphi_{\mathbf{k}_f}(\mathbf{r}_1) = \frac{1}{2}k_f^2\varphi_{\mathbf{k}_f}(\mathbf{r}_1). \tag{55}$$

For the present purpose, we set the distorting potential $U_f(r_1) = -(Z_N - 1)/r_1$ such that the scattered outgoing electron is described by a Coulomb wave.

The final excited state $\phi_f(\mathbf{r}_2)$ satisfies

$$\left(-\frac{1}{2}\nabla_2^2 - \frac{Z_N}{r_2} - \varepsilon_n\right)\phi_f(\mathbf{r}_2) = 0 \tag{56}$$

where $\varepsilon_n = -0.5Z_N^2/n^2$ is the energy of the excited state.

The T-matrix element for a transition from an initial state to a final state is then given by

$$f_{exci} = \langle \varphi^{-}_{\mathbf{k}_f}(\mathbf{r}_1)\phi_f(\mathbf{r}_2)|V_i|\varphi_{\mathbf{k}_i}(\mathbf{r}_1)\phi_i(\mathbf{r}_2)\rangle, \tag{57}$$

where V_i is given by Eq. (46). The differential cross section (DCS) for this transition is given by

$$\frac{d\sigma_{exci}}{d\Omega} = (2\pi)^4\frac{k_f}{k_i}\left(\frac{3}{4}|f_{exci} - g_{exci}|^2 + \frac{1}{4}|f_{exci} + g_{exci}|^2\right) \tag{58}$$

where the exchange amplitude g_{exci} is calculated from

$$g_{exci} = \langle \varphi^{-}_{\mathbf{k}_f}(\mathbf{r}_2)\phi_f(\mathbf{r}_1)|V_i|\varphi_{\mathbf{k}_i}(\mathbf{r}_1)\phi_i(\mathbf{r}_2)\rangle. \tag{59}$$

The (e,2e) and the excitation cross sections presented here are for the collisions of free electrons with an atomic ion. In the collisions by the rescattering electrons with the parent ion, one should preserve the spin of the total system. Thus if the target is helium, for example, the total spin of the returning electron and the target He^+ ion should be spin singlet. In this case, the triplet contributions in Eqs. (53) and (58) should be dropped.

2.9 Laser-induced medium energy electron diffraction of molecules

The scattering theories presented here are mostly for atomic targets. Similar theories can be and have been generalized to molecular targets. In most cases, electron scattering or photoionization of molecules are rather complicated and will not be described here. With the additional degrees of freedom for molecules, such calculation

would be very time consuming. However, there are situations where such calculations are quite simple. It is the so-called Independent Atom Model (IAM). In IAM, a molecule is modeled as consisting of a collection of individual atoms fixed at $\mathbf{R}_i$. Let f_i be the complex scattering amplitude of the i^{th} atom alone, according to IAM, the total scattering amplitude for a molecule fixed-in-space can be expressed as

$$F(k,\theta,\varphi;\Omega_L) = \sum_i f_i e^{i\mathbf{q}\cdot\mathbf{R}_i}, \tag{60}$$

where Ω_L is the angle between the molecular axis with respect to the direction of the incident electron, and $\mathbf{q} = \mathbf{k} - \mathbf{k}_0$ is the momentum transfer. The incident electron momentum $\mathbf{k}_0$ is taken to be along the z-axis. The scattering cross section is then given by

$$I_{tot}(\theta,\varphi;\Omega_L) = I_A + \sum_{i\neq j} f_i f_j^* e^{i\mathbf{q}\cdot\mathbf{R}_{ij}}, \tag{61}$$

where $\mathbf{R}_{ij} = \mathbf{R}_i - \mathbf{R}_j$, and $I_A = \sum_i |f_i|^2$. Here I_A is the incoherent sum of scattering cross sections from all the atoms in the molecule. The second term, I_M, is the molecular interference term. For electron scattering from a sample of randomly distributed molecules, the above expression is averaged over Ω_L, and

$$\langle I_{tot}\rangle(\theta) = I_A + \sum_{i\neq j} f_i f_j^* \frac{\sin(qR_{ij})}{qR_{ij}} \tag{62}$$

in which q and R_{ij} are the moduli of $\mathbf{q}$ and $\mathbf{R}_{ij}$, respectively. It is interesting to note that the molecular interference term does not vanish after the average, as pointed out by Fano and Cohen in 1967 [14]. According to IAM, we can define the molecular contrast factor (MCF) as

$$\gamma = \frac{1}{I_A}\sum_{i\neq j} f_i f_j^* \frac{\sin(qR_{ij})}{qR_{ij}}. \tag{63}$$

In the traditional gas-phase electron diffraction (GED) where molecules are randomly distributed, an inverse sine transform was used to derive the interatomic separation distributions from Eq. (62). In GED, typical incident electrons have energies in the tens and hundreds of keV, and the scattered electrons are collected in the forward directions. From Section 2.4, for HATI spectra, clearly the DCS can be extracted from the photoelectron momentum spectra generated by infrared lasers. However, the returning electron for a molecule in a laser field with Ponderomotive energy U_p can only reach a maximum energy of about 3.2 U_p. For typical 800 nm Ti-Sa lasers, the returning electrons have energies near or below 50 eV. Thus the standard GED theory cannot be applied. However, as shown in Fig. 3, the DCS of CO_2 at large angles are well-described by the IAM model for incident electron energies above about 50 eV, for molecules that are randomly distributed. The results in Fig. 3 indicates that DCS extracted from the HATI spectra for molecular targets may be used to obtain the target information if the returning electron energies are above

50 eV. Such returning energies can be easily achieved using mid-infrared (MIR) lasers. Since the IAM is the basis of the GED, this implies that molecular structure can also be retrieved from diffraction images generated by MIR lasers. This further implies that MIR lasers can be used to study the time-dependent structural change of a molecule. The temporal resolution of such measurement is determined by the pulse durations which are in the order of few femtoseconds. Further development of dynamic chemical imaging of molecules with infrared lasers is awaiting for HATI electron spectra from aligned molecules.

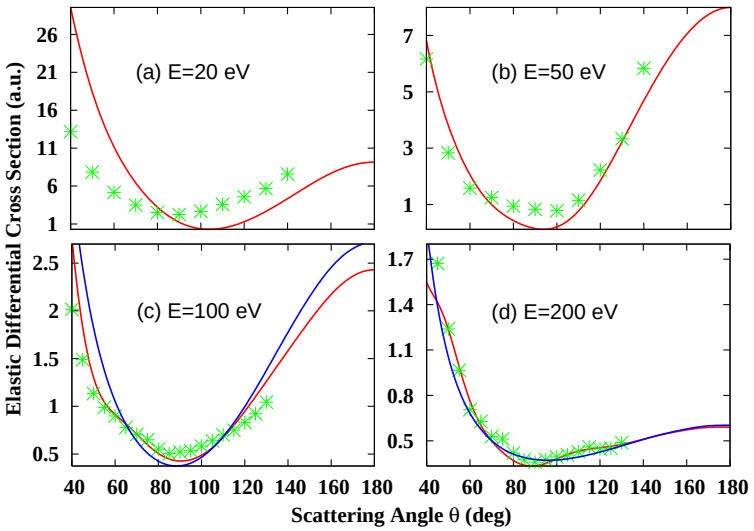

Fig. 3 Elastic scattering cross sections at large angles between electrons and isotropically distributed CO_2 molecules. The experimental data [15, 16] are compared to the theoretical prediction of the Independent Atom Model, showing poor agreement at 20 eV, but general good agreement at higher collision energies.

3 Summary

In this Chapter we summarize the elements of basic scattering theory for dynamic chemical imaging with infrared lasers. These scattering theories have been developed in the conventional energy domain physics for studying the structure of atoms and molecules. Based on the quantitative rescattering (QRS) theory we demonstrated that the same field-free collision theory can be used for describing time-resolved studies of transient atomic and molecular systems. Clearly, even for the time-dependent systems, experimentally it is the energy, momentum or charge of the atomic and molecular systems that are measured. By taking advantage of the

basic scattering theories developed over the years directly for the study of time-dependent systems, one does not need to develop all the new tools for studying quantum imaging problems. In the meanwhile, by utilizing the coherent nature of the returning electron wave packet or the coherent harmonic light sources, studies in ultrafast atomic and molecular processes would reveal new features that cannot be revealed in the conventional energy-domain studies.

References

1. Hargittai I and Hargittai M 1988 *Stereochemical Applications of Gas-Phase Electron Diffraction*, (VCH, New York), and references therein
2. Zewail A H and Thomas J M 2009 *4D Electron Microscopy: Imaging in Space and Time* (Imperial College)
3. Corkum P B 1993 Phys. Rev. Lett. **71** 1994
4. Krause J L, Schafer K J and Kulander K C 1993 Phys. Rev. Lett. **68** 3535
5. Morishita T, Le A T, Chen Zhangjin and Lin C D 2008 Phys. Rev. Lett. **100** 013903
6. Lin C. D., Le A T, Chen Zhangjin, Morishita T and Lucchese R, J. Phys. B **43**, 122001 (2010).
7. Chen Zhangjin, Morishita T, Le A T, Wickenhauser M, Tong X M and Lin C D 2006 Phys. Rev. A **74** 053405
8. Becker W *et al* 2002 *Adv. At. Mol. Opt. Phys.* **48** 35
9. Hasovic E, Busuladžić M, Gazibegović-Busuladžić A, Milošević D B and Becker
10. Chen Zhangjin, Morishita T, Le A T and Lin C D 2007 Phys. Rev. A **76** 043402
11. Morishita T, Chen Zhangjin, Watanabe S and Lin C D 2007 Phys. Rev. A **75** 023407
12. Le A T, Lucchese R R, Tonzani S, Morishita T and Lin C D 2009 Phys. Rev. A **80** 013401
13. Brauner M, Briggs J S, and Klar H, J. Phys. B **22**, 2265 (1989).
14. Cohen H D and Fano U 1966 *Phys. Rev.* **150** 30
15. Register D F, Nishimura H and Trajmar 1980 J. Phys. B **13** 1651
16. Iga I, Homem M G, Mazon K T and Lee M T 1999 J. Phys. B **32** 4373